Nd3+-activated CaF2 ceramic lasers

journal or publication title	Optics Letters
volume	44
number	13
page range	3378-3381
year	2019
URL	http://hdl.handle.net/10655/00013030

doi: 10.1364/OL.44.003378

Nd^{3+}-activated CaF_2 ceramic lasers

H. CHEN,[1] A. IKESUE,[2] H. NOTO,[1,3] H. UEHARA,[1,3] Y. HISHINUMA,[1,3] T. MUROGA,[1,3] AND R. YASUHARA[1,3,*]

[1] *National Institute for Fusion Science, 322-6 Oroshi-cho, Toki, Gifu, Japan*
[2] *World-Lab. Co., Ltd., Mutsuno, Atsutaku, Nagoya 456-0023, Japan*
[3] *SOKENDAI (The Graduate University for Advanced Studies), 322-6 Oroshi-cho, Toki, Gifu, Japan*
**Corresponding author: yasuhara.ryo@nifs.ac.jp*

Received XX Month XXXX; revised XX Month, XXXX; accepted XX Month XXXX; posted XX Month XXXX (Doc. ID XXXXX); published XX Month XXXX

Nd,Y:CaF_2 and Nd,La:CaF_2 ceramics featuring good optical quality have been fabricated by reactive sintering and hot isostatic pressing method. The transmission spectra, emission spectra, and fluorescence decay curves were measured. Lasing at 1064 nm and 1065 nm were observed in Nd,Y:CaF_2 and Nd,La:CaF_2, respectively, upon quasi-continuous-wave pumping by a diode laser emitting at 791 nm. This is the first demonstration of Nd^{3+}-activated CaF_2 ceramic laser to the best of our knowledge.

http://dx.doi.org/10.1364/OL.99.099999

CaF_2 has been extensively studied as laser host material due to its high thermal conductivity (9.7 $W{\cdot}m^{-1}{\cdot}K^{-1}$), low phonon energy (~495 cm^{-1}), and low nonlinear refractive coefficient [1–3]. More importantly, doping trivalent rare-earth ions in this matrix leads to inhomogeneous spectral broadening due to heterovalent substitution of the Ca^{2+} site [4]. The broad spectral linewidth of RE^{3+}:CaF_2 is favorable for ultrashort pulse generation. For example, 99-fs mode-locked pulses can be produced by an Yb:CaF_2 single crystal. In the case of Nd^{3+}, however, this ion tends to aggregate and form [Nd^{3+}-Nd^{3+}] clusters in the CaF_2 host, which intensify the cross-relaxation processes and quench the luminescence [5]. This detrimental effect can be weakened by codoping buffer ions such as Y^{3+}, La^{3+}, and Lu^{3+} that are able to break the [Nd^{3+}-Nd^{3+}] clusters [6]. It is also worth noting that, the introduction of RE^{3+} buffer ions can further broaden the spectral linewidth of the active ions [7]. In 2014, Z. P. Qin et al. reported mode-locked operation using a Nd,Y:CaF_2 crystal featuring an ultrashort pulse duration of 103 fs, which is the shortest pulse produced by a Nd^{3+}-doped single crystal at that moment [8]. This impressive result suggests that the Nd,RE:CaF_2 materials are promising gain media for ultrafast lasers. In addition, continuous-wave [6,9–12], Q-switched [12,13], and mode-locked [9,14] operations of Nd,Y:CaF_2, Nd,La:CaF_2 or Nd,Lu:CaF_2 crystal lasers have been documented.

Although the Nd^{3+}-activated CaF_2 crystal lasers have been well studied, laser oscillation based on ceramic samples has not been reported to date. In fact, the first ceramic laser was realized by Dy:CaF_2 [15]. Moreover, efficient CaF_2 ceramic lasers have been achieved by other lanthanide active ions such as Yb^{3+} and Er^{3+} [16,17]. It is known that the ceramic materials feature several advantages over single crystals as gain media, including lower production costs, better thermo-mechanical resistance, and the potential to build designated composites [18]. This motivates us to study Nd^{3+}-activated CaF_2 ceramics for laser applications.

In this paper, we report the synthesis, optical spectroscopic characterization, and laser operation of two ceramic materials, 1 at.%Nd, 1.8 at.%Y:CaF_2 and 1 at.%Nd, 2 at.%La:CaF_2 (hereafter denoted as Nd,Y:CaF_2 and Nd,La:CaF_2 for conciseness). The spectroscopic properties related to the laser performance, viz. transmission spectra, emission spectra, and fluorescence lifetime will be presented. Lasing of these Nd^{3+}-activated CaF_2 ceramics is demonstrated for the first time. The cavity setup and lasing behavior will be discussed.

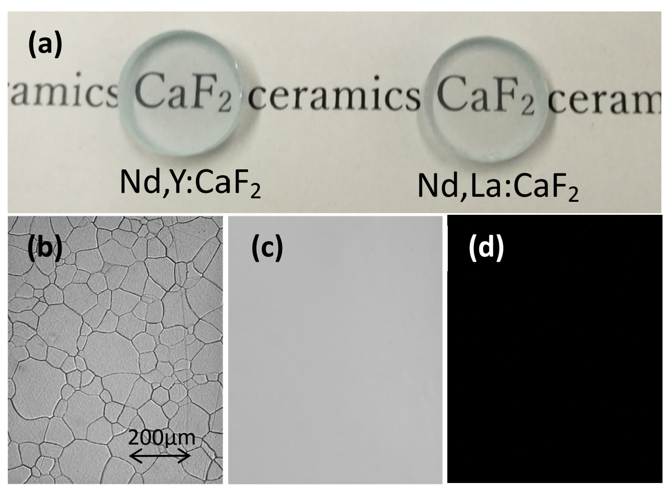

Fig. 1. (a) Photograph of Nd,Y:CaF_2 and Nd,La:CaF_2 transparent ceramics under ambient light; (b) Reflection microscope image of Nd,La:CaF_2; Transmission microscope image of Nd,La:CaF_2 under open (c) and crossed (d) nicols.

The Nd,Y:CaF_2 and Nd,La:CaF_2 ceramics were fabricated by hot isostatic pressing (HIP) method. The high-purity fluoride compounds CaF_2 (3 µm particle size, >3N purity), NdF_3 (0.6 µm particle size, 4N purity), and LaF_3/YF_3 (0.3 µm particle size, 3N purity) were used as starting materials. The raw materials were ball milled in ethanol. A spray dryer was then used to dry the slurry and granulate the mixed powders. The granulated powders (~30 µm) were pressed into disks with metal molds, followed by cold isostatic press at 147 MPa. The obtained powder compacts were presintered at 1000°C for 2 hours under nitrogen atmosphere and then isostatically pressed at 1100°C for 3 hours under argon (176 MPa), using the HIP facilities at National Institute for Fusion Science. The as-synthesized ceramic samples were polished on both sides.

A photograph of the polished Nd,Y:CaF_2 and Nd,La:CaF_2 ceramics (Φ12 mm × 3 mm) is shown in Fig. 1(a). Both samples exhibit good transparency. A polarized optical microscope was used to observe the microstructure of the Nd,La:CaF_2 ceramic. It can be seen from the reflection microscopic image (Fig. 1(b)) that the grain size varies from ca. 50 to 200 µm and no noticeable residual pores can be detected on the surface. Only a few residual pores (<1µm) can be observed with the transmitted microscope. The optical isotropy of this ceramic was verified by the polarized transmission microscope images (Fig. 1(c) and (d)), in which birefringence was not observed.

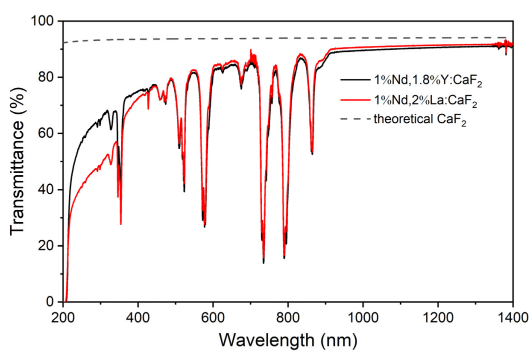

Fig. 2. Transmission spectra of Nd,Y:CaF_2 and Nd,La:CaF_2 ceramics.

Fig. 2 shows the transmission spectra (200-1400 nm) of Nd,Y:CaF_2 and Nd,La:CaF_2 ceramics measured with a SHIMADZU UV-3600Plus spectrophotometer at room temperature. The Fresnel transmittance of CaF_2 is given in the figure as reference. The transmittance at 1064 nm, which is the potential lasing wavelength, of Nd,Y:CaF_2 and Nd,La:CaF_2 were measured to be 90% and 91%, respectively. These values are superior to the reported values of a 2-mm-thick 5% Nd:CaF_2 ceramic (~88%, Ref. [19]) and a 2-mm-thick 1% Nd, 1%La:CaF_2 ceramic (~88%, Ref. [20]) prepared by hot pressing method. Comparison to the theoretical transmittance value of 94% results in optical losses of 4% and 3% at the 1µm region in Nd,Y:CaF_2 and Nd,La:CaF_2, respectively. The relatively good optical transmittance of these two ceramics indicate that they are more probable to lase than the currently reported analogous ceramics. Nevertheless, a decrease of transmittance values at shorter wavelengths was observed as well, which is due to typical Rayleigh scattering. Improvement of the optical quality in this class of ceramics, by means of optimizing the synthesis technique and microstructure, still remains a research topic. In addition, according to the transmission spectra, the peak wavelengths of the potential pump transitions of $^4I_{9/2}\rightarrow{}^4F_{5/2}+{}^2H_{9/2}$ are found to be around 790 nm with a shoulder peak around 795 nm for both materials.

The fluorescence spectra of Nd,Y:CaF_2 and Nd,La:CaF_2 were recorded at room temperature (ADVANTEST Q9381A optical spectrum analyzer) under excitation at 791 nm. The obtained spectra were calibrated to relative irradiance and converted to emission cross-sections via Füchtbauer-Ladenburg equation [21]:

$$\sigma_{em}(\lambda) = \frac{\lambda^5 I(\lambda)}{8\pi n^2 c\tau_{rad}\int \lambda I(\lambda)d\lambda}$$

where $I(\lambda)$ is the spectral irradiance, c is the velocity of light, n is the refractive index of the medium, and τ_{rad} is the radiative lifetime of the $^4F_{3/2}$ manifold. The wavelength-dependent refractive index of pure CaF_2 and the radiative lifetime of the 1%Nd, 2%Y:CaF_2 single crystal reported in Ref. [10] (0.5 ms, obtained by Judd-Ofelt analysis) were used for the calculation of emission cross-sections. The weak $^4F_{3/2}\rightarrow{}^4I_{15/2}$ transition could be omitted for the calculation thus the integration was made from 825 to 1450 nm.

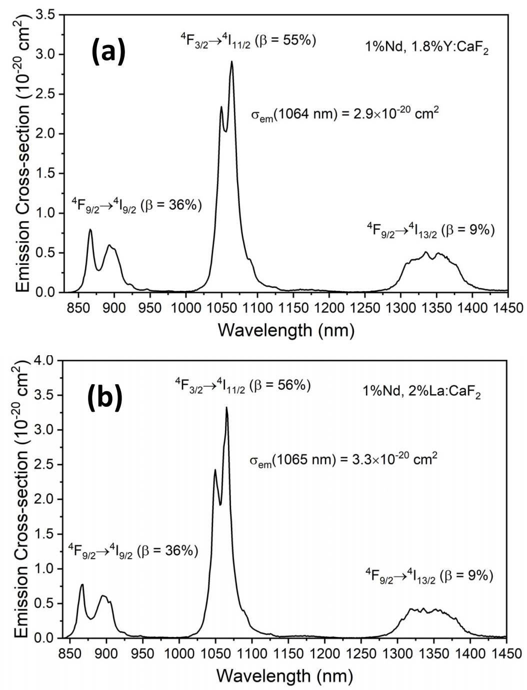

Fig. 3. Emission cross-section spectra of (a) Nd,Y:CaF_2 ceramic and (b) Nd,La:CaF_2 ceramic.

The resulting emission spectra are presented in Fig. 3. The three broad emission bands, resulting from the disordered structure in these Nd,RE:CaF_2 matrices, can be assigned to the $^4F_{3/2}\rightarrow{}^4I_{9/2}$, $^4I_{11/2}$, and $^4I_{13/2}$ transitions as marked in the figure and their experimental branching ratios are found to be ca. 36%, 55%, and 9% for both materials, respectively. These values are comparable to the corresponding branching ratios of a 1%Nd, 2%Y:CaF_2 single crystal, which are 37%, 52%, and 11% [10]. The spectral line shapes of Nd,Y:CaF_2 and Nd,La:CaF_2 are slightly different. The former peaks at 1064 nm, giving an emission cross-section of 2.9× 10^{-20} cm^2, while the latter shows the largest cross-section at 1065 nm, which is ca. 3.3×10^{-20} cm^2. The peak emission cross-section of the Nd,Y:CaF_2 ceramic is close to that of a 1%Nd, 2%Y:CaF_2 single crystal as well, which is 2.8×10^{-20} cm^2 [10].

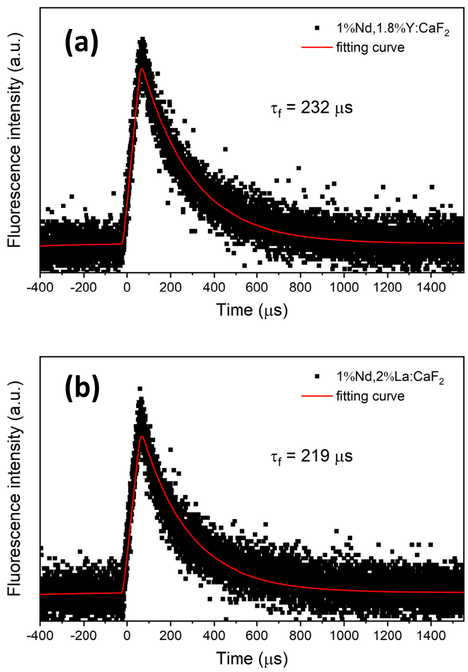

Fig. 4. Fluorescence decay profiles of (a) Nd,Y:CaF_2 ceramic and (b) Nd,La:CaF_2 ceramic under pulsed (100 μs) excitation at 791 nm.

As is stated above, the Nd:CaF_2 compound suffers from formation of [Nd^{3+}-Nd^{3+}] clusters and, consequently, a short fluorescence lifetime. Thus it is essential to examine the fluorescence dynamics in these Nd^{3+}-doped CaF_2 ceramics. Fluorescence decay curves of the Nd,Y:CaF_2 and Nd,La:CaF_2 ceramics were recorded at room temperature to derive the fluorescence lifetime. The samples were excited by 791-nm laser pulses with pulse duration of 100 μs. The temporal evolution of the fluorescence intensity was detected by a Thorlabs DET36A/M Silicon Detector (rise time 14 ns, equipped with a 1-μm longpass filter) and recorded with an oscilloscope (data interval 200 ns). The waveform of the excitation pulse was measured as well in order to deconvolute the obtained decay curves. The resulting curves of both samples exhibit a single-exponential decay behavior (Fig. 4, both fittings give chi square = 0.002) and the fluorescence lifetimes from the $^4F_{3/2}$ manifold were calculated to be 232 μs and 219 μs for Nd,Y:CaF_2 and Nd,La:CaF_2, respectively. Due to the introduction of Y^{3+} or La^{3+} buffer ions, the fluorescence lifetimes are one order of magnitude larger than that measured with a 1%Nd:CaF_2 ceramic, which is ca. 15 μs [22]. In addition, these values are similar to that measured by a 1%Nd, 2%Y:CaF_2 single crystal (208 μs, Ref. [10]). This indicates that the fabricated ceramics are free from remarkable quenching centers.

Owing to the favorable spectroscopic properties of the fabricated Nd,Y:CaF_2 and Nd,La:CaF_2 ceramics, preliminary laser experiments were conducted for lasing the most intense $^4F_{3/2}\rightarrow{}^4I_{11/2}$ transition around 1064 nm using a typical plano-concave cavity. The setup for the laser experiments is schematically shown in Fig. 5. A multi-mode fiber-coupled (core diameter 100 μm, NA = 0.22) laser diode (Han's TCS, M793±3-16-F105/22-C1-P) was used for pumping. The peak wavelengths of the pump emission vary from 791 to 792 nm in this demonstration, depending on the output power. A pair of plano-convex lenses with focal length of 50 mm were employed for collimation and focusing. Since the ceramics were only allowed for air-cooling at the moment, the laser diode was operated in quasi-cw mode so as to lessen the thermal load. Pump laser pulses with 1 ms duration and 50 Hz repetition rate (5% duty cycle) were generated by the driving system. The input coupler is anti-reflection coated at the pump wavelength and high-reflection coated at the lasing wavelength. The output coupler has a radius of curvature of 50 mm and 2% transmittance from 1000 to 1100 nm. The ceramic samples (without any coating) were placed as close as possible to the input mirror. The optimal cavity length in this configuration was found to be 40 mm.

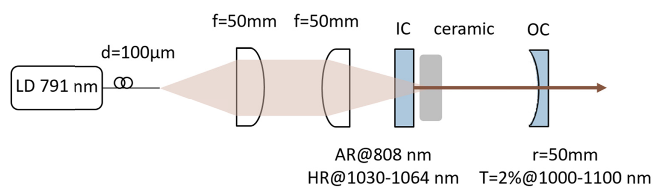

Fig. 5. Setup for the Nd^{3+}-activated CaF_2 ceramic lasers.

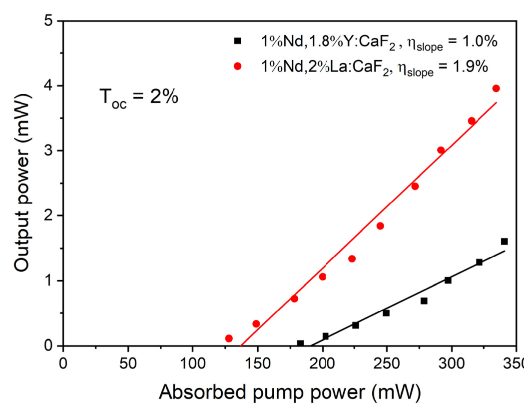

Fig. 6. Dependence of the average output power on the absorbed pump power under quasi-cw pumping.

The average pump and output (passed through a 1-μm longpass filter) power was recorded by a Thorlabs PM160T power meter. The absorption efficiencies of the pump power were measured to be around 78% and 77% in Nd,Y:CaF_2 and Nd,La:CaF_2, respectively. The decent absorption efficiencies result from the good spectral overlap between the absorption bands and the pump emission (790 nm vs. 791 nm). The lasing threshold power of Nd,Y:CaF_2 and Nd,La:CaF_2 were measured to be 180 mW and 130 mW, respectively, corresponding to 3.7 W and 2.6 W in the ideal case of continuous-wave pumping. The input-output characteristics of these two ceramics lasers are illustrated in Fig. 6. The slope efficiencies are fitted to be 1.0% for Nd,Y:CaF_2 and 1.9% for Nd,La:CaF_2. The typical spectra (Ocean Optics HR4000, 0.12 nm resolution) of the free-running Nd^{3+}-activated CaF_2 ceramic lasers are presented in Fig. 7. The center wavelengths of the oscillation lines, viz. 1064 nm for Nd,Y:CaF_2 and 1065 nm for Nd,La:CaF_2, are in line with the emission spectroscopic data. Compare to the laser performance of the CaF_2 lasers based on single crystals (e.g. 0.5%Nd, 2%La:CaF_2 with lasing threshold less than 0.5 W and slope efficiency of 40%, Ref. [23]), the high lasing thresholds and low efficiencies of these two lasers can be attributed to the optical losses of the ceramics at the lasing wavelength (4% in Nd,Y:CaF_2 and 3% in Nd,La:CaF_2), despite the fact that these values are smaller than those of the other reported Nd^{3+}-doped CaF_2 ceramics [19,20]. In addition, since the two ceramics have comparable fluorescence lifetimes, the larger threshold pump power and the smaller slope efficiency of Nd,Y:CaF_2 than Nd,La:CaF_2 are probably related to the greater optical losses of the former. We believe that better laser performance can be achieved by further improving the optical quality of the ceramic gain material (e.g. grain boundaries and index homogeneity) and by optimizing the laser cavity design, such as applying anti-reflection coating for the ceramic samples and varying the output-coupler transmission.

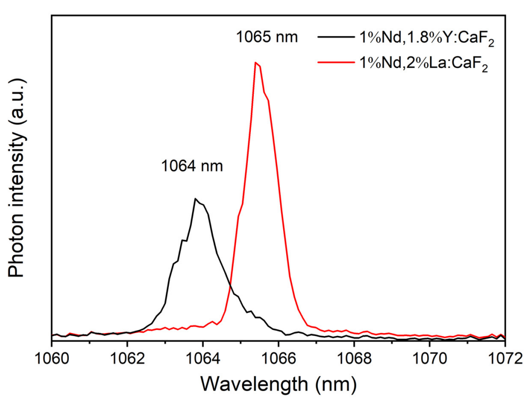

Fig. 7. Laser emission spectra of Nd,Y:CaF_2 and Nd,La:CaF_2.

In conclusion, we have fabricated two Nd^{3+}-activated CaF_2 ceramics, 1 at.%Nd, 1.8 at.%Y:CaF_2 and 1 at.%Nd, 2 at.%La:CaF_2, by HIP method and studied their optical spectroscopic as well as laser properties. The Nd,La:CaF_2 ceramic exhibits no noticeable residual pores and favorable optical homogeneity. The transmittance at the lasing wavelength is up to 90% in both materials, which exceeds the other reported analogous ceramics. The emission spectroscopic properties, including the emission cross-sections and fluorescence lifetime, are comparable to the reported values of a single crystal with a similar composition. Owing to their relatively good optical quality, we have succeeded in laser oscillation using Nd^{3+}-activated CaF_2 ceramic media for the first time to our knowledge. In the preliminary laser operation of Nd,Y:CaF_2 and Nd,La:CaF_2, the lasing wavelengths were found to be 1064 nm and 1065 nm, and the slope efficiencies were 1.0% and 1.9% , respectively. Works on enhancing the efficiency of the Nd^{3+}-activated CaF_2 ceramic lasers are already in progress, including optimizing the composition as well as the synthesis technique of the ceramic materials, installing a water-cooling system for the ceramics, and optimizing the cavity configuration.

Funding. Japan Society for the Promotion of Science (JSPS) (18H01204 and 15KK0245).

Acknowledgment. This work was performed with the support and under the auspices of the National Institute for Fusion Science Research program (ULHH040 and URSX204).

References

1. V. Petit, J. L. Doualan, P. Camy, V. Ménard, and R. Moncorgé, Appl. Phys. B **78**, 681 (2004).
2. Z. Zhang, X. Guo, J. Wang, C. Zhang, J. Liu, and L. Su, Opt. Lett. **43**, 4300 (2018).
3. P. Aballea, A. Suganuma, F. Druon, J. Hostalrich, P. Georges, P. Gredin, and M. Mortier, Optica **2**, 288 (2015).
4. C. R. A. Catlow, A. V. Chadwick, G. N. Greaves, and L. M. Moroney, Nature **312**, 601 (1984).
5. S. A. Payne, J. A. Caird, L. L. Chase, L. K. Smith, N. D. Nielsen, and W. F. Krupke, J. Opt. Soc. Am. B **8**, 726 (1991).
6. J. L. Doualan, L. B. Su, G. Brasse, A. Benayad, V. Ménard, Y. Y. Zhan, A. Braud, P. Camy, J. Xu, and R. Moncorgé, J. Opt. Soc. Am. B **30**, 3018 (2013).
7. Q. Wang, L. Su, F. Ma, Y. Zhan, D. Jiang, X. Qian, J. Wang, L. Zheng, J. Xu, W. Ryba-Romanowski, P. Solarz, and R. Lisiecki, Opt. Mater. **36**, 455 (2013).
8. Z. P. Qin, G. Q. Xie, J. Ma, W. Y. Ge, P. Yuan, L. J. Qian, L. B. Su, D. P. Jiang, F. K. Ma, Q. Zhang, Y. X. Cao, and J. Xu, Opt. Lett. **39**, 1737 (2014).
9. C. Li, F. Zhang, J. Liu, L. Su, D. Jiang, J. Liu, J. Liu, and J. Xu, Opt. Mater. Express **5**, 1972 (2015).
10. D. Jiang, Y. Zhan, Q. Zhang, F. Ma, L. Su, F. Tang, X. Qian, and J. Xu, CrystEngComm **17**, 7398 (2015).
11. L. B. Su, Q. G. Wang, H. J. Li, G. Brasse, P. Camy, J. L. Doualan, A. Braud, R. Moncorgé, Y. Y. Zhan, L. H. Zheng, X. B. Qian, and J. Xu, Laser Phys. Lett. **10**, 035804 (2013).
12. C. Li, M. Fan, J. Liu, L. Su, D. Jiang, X. Qian, and J. Xu, Opt. Laser Techno. **69**, 140 (2015).
13. Q. Hao, S. Pang, J. Liu, and L. Su, Appl. Opt. **57**, 6491 (2018).
14. H. Wang, J. Zhu, Z. Gao, Y. Yu, K. Liu, J. Wang, Z. Wei, J. Liu, D. Jiang, F. Ma, and L. Su, Opt. Mater. Express **6**, 2184 (2016).
15. S. E. Hatch, W. F. Parsons, and R. J. Weagley, Appl. Phys. Lett. **5**, 153 (1964).
16. S. Kitajima, K. Yamakado, A. Shirakawa, K. Ueda, Y. Ezura, and H. Ishizawa, Opt. Lett. **42**, 1724 (2017).
17. W. Ma, L. Su, X. Xu, J. Wang, D. Jiang, L. Zheng, X. Fan, C. Li, J. Liu, and J. Xu, Opt. Mater. Express **6**, 409 (2016).
18. A. Ikesue and Y. L. Aung, Nat. Photonics **2**, 721 (2008).
19. G. Lu, B. Mei, J. Song, W. Li, and R. Xing, Mater. Lett. **115**, 162 (2014).
20. X. Xie, B. Mei, J. Song, W. Li, and L. Su, Opt. Mater. **76**, 111 (2018).
21. D. E. McCumber, Phys. Rev. **136**, A954 (1964).
22. Z. Sun, B. Mei, W. Li, Z. Liu, and L. Su, J. Am. Ceram. Soc. **99**, 4039 (2016).
23. S. Wang, D. Jiang, Q. Wu, Z. Cao, S. Pang, J. Wang, X. Qian, J. Liu, B. Mei, and L. Su, Laser Phys. **29**, 015801 (2018).

Full References

1. V. Petit, J. L. Doualan, P. Camy, V. Ménard, and R. Moncorgé, "CW and tunable laser operation of Yb^{3+} doped CaF_2," Appl. Phys. B **78**, 681–684 (2004).
2. Z. Zhang, X. Guo, J. Wang, C. Zhang, J. Liu, and L. Su, "High-efficiency 2 μm continuous-wave laser in laser diode-pumped Tm^{3+}, La^{3+}: CaF_2 single crystal," Optics Letters **43**, 4300 (2018).
3. P. Aballea, A. Suganuma, F. Druon, J. Hostalrich, P. Georges, P. Gredin, and M. Mortier, "Laser performance of diode-pumped Yb:CaF_2 optical ceramics synthesized using an energy-efficient process," Optica **2**, 288 (2015).
4. C. R. A. Catlow, A. V. Chadwick, G. N. Greaves, and L. M. Moroney, "Direct observations of the dopant environment in fluorites using EXAFS," Nature **312**, 601 (1984).
5. S. A. Payne, J. A. Caird, L. L. Chase, L. K. Smith, N. D. Nielsen, and W. F. Krupke, "Spectroscopy and gain measurements of Nd^{3+} in SrF_2 and other fluorite-structure hosts," J. Opt. Soc. Am. B, JOSAB **8**, 726–740 (1991).
6. J. L. Doualan, L. B. Su, G. Brasse, A. Benayad, V. Ménard, Y. Y. Zhan, A. Braud, P. Camy, J. Xu, and R. Moncorgé, "Improvement of infrared laser properties of Nd:CaF_2 crystals via codoping with Y^{3+} and Lu^{3+} buffer ions," J. Opt. Soc. Am. B, JOSAB **30**, 3018–3021 (2013).
7. Q. Wang, L. Su, F. Ma, Y. Zhan, D. Jiang, X. Qian, J. Wang, L. Zheng, J. Xu, W. Ryba-Romanowski, P. Solarz, and R. Lisiecki, "Nd^{3+}:CaF_2 crystal with controlled photoluminescence spectroscopic properties by codoping Y^{3+} ions," Optical Materials **36**, 455–457 (2013).
8. Z. P. Qin, G. Q. Xie, J. Ma, W. Y. Ge, P. Yuan, L. J. Qian, L. B. Su, D. P. Jiang, F. K. Ma, Q. Zhang, Y. X. Cao, and J. Xu, "Generation of 103 fs mode-locked pulses by a gain linewidth-variable Nd,Y:CaF_2 disordered crystal," Optics Letters **39**, 1737 (2014).
9. C. Li, F. Zhang, J. Liu, L. Su, D. Jiang, J. Liu, J. Liu, and J. Xu, "Continuous-wave and mode-locked operation of a diode-pumped Nd,La:CaF_2 laser," Optical Materials Express **5**, 1972 (2015).
10. D. Jiang, Y. Zhan, Q. Zhang, F. Ma, L. Su, F. Tang, X. Qian, and J. Xu, "Nd,Y:CaF_2 laser crystals: novel spectral properties and laser performance from a controlled local structure," CrystEngComm **17**, 7398–7405 (2015).
11. L. B. Su, Q. G. Wang, H. J. Li, G. Brasse, P. Camy, J. L. Doualan, A. Braud, R. Moncorgé, Y. Y. Zhan, L. H. Zheng, X. B. Qian, and J. Xu, "Spectroscopic properties and CW laser operation of Nd, Y-codoped CaF_2 single crystals," Laser Physics Letters **10**, 035804 (2013).
12. C. Li, M. Fan, J. Liu, L. Su, D. Jiang, X. Qian, and J. Xu, "Operation of continuous wave and Q-switching on diode-pumped Nd,Y:CaF_2 disordered crystal," Optics & Laser Technology **69**, 140–143 (2015).
13. Q. Hao, S. Pang, J. Liu, and L. Su, "Tunable and passively Q-switched laser operation of Nd,Lu:CaF_2 disordered crystal," Appl. Opt., AO **57**, 6491–6495 (2018).
14. H. Wang, J. Zhu, Z. Gao, Y. Yu, K. Liu, J. Wang, Z. Wei, J. Liu, D. Jiang, F. Ma, and L. Su, "Femtosecond mode-locked Nd,La:CaF_2 disordered crystal laser," Optical Materials Express **6**, 2184 (2016).
15. S. E. Hatch, W. F. Parsons, and R. J. Weagley, "HOT-PRESSED POLYCRYSTALLINE CaF_2:Dy^{2+} LASER," Appl. Phys. Lett. **5**, 153–154 (1964).
16. S. Kitajima, K. Yamakado, A. Shirakawa, K. Ueda, Y. Ezura, and H. Ishizawa, "Yb^{3+}-doped CaF_2-LaF_3 ceramics laser," Optics Letters **42**, 1724 (2017).
17. W. Ma, L. Su, X. Xu, J. Wang, D. Jiang, L. Zheng, X. Fan, C. Li, J. Liu, and J. Xu, "Effect of erbium concentration on spectroscopic properties and 2.79 μm laser performance of Er:CaF_2 crystals," Opt. Mater. Express, OME **6**, 409–415 (2016).
18. A. Ikesue and Y. L. Aung, "Ceramic laser materials," Nature Photonics **2**, 721–727 (2008).
19. G. Lu, B. Mei, J. Song, W. Li, and R. Xing, "Fabrication and properties of highly transparent Nd-doped CaF_2 ceramics," Materials Letters **115**, 162–164 (2014).
20. X. Xie, B. Mei, J. Song, W. Li, and L. Su, "Fabrication and spectral properties of Nd, La: CaF_2 transparent ceramics," Optical Materials **76**, 111–116 (2018).
21. D. E. McCumber, "Einstein Relations Connecting Broadband Emission and Absorption Spectra," Physical Review **136**, A954–A957 (1964).
22. Z. Sun, B. Mei, W. Li, Z. Liu, and L. Su, "Effects of Nd Concentration on Microstructure and Optical Properties of Nd: CaF_2 Transparent Ceramics," Journal of the American Ceramic Society **99**, 4039–4044 (2016).
23. S. Wang, D. Jiang, Q. Wu, Z. Cao, S. Pang, J. Wang, X. Qian, J. Liu, B. Mei, and L. Su, "Effect of La^{3+} proportion on spectroscopic and continuous wave laser properties of Nd, La: CaF_2 single crystals." Laser Physics **29**, 015801 (2018).